Corrosion Science 53 (2011) 2419–2429

Contents lists available at ScienceDirect

Corrosion Science

journal homepage: www.elsevier.com/locate/corsci

Influence of the applied stress rate on the stress corrosion cracking of 4340 and 3.5NiCrMoV steels under conditions of cathodic hydrogen charging

S. Ramamurthy [a,b,*], W.M.L. Lau [b], A. Atrens [a]

[a] Division of Materials, School of Engineering, University of Queensland, St. Lucia, QLD 4072, Australia
[b] Surface Science Western, The University of Western Ontario, London, Ontario, Canada N6G 0J3

ARTICLE INFO

Article history:
Received 25 December 2009
Accepted 29 March 2011
Available online 2 April 2011

Keywords:
A. Steel
C. Hydrogen embrittlement
C. Stress corrosion

ABSTRACT

Stress corrosion cracking (SCC) of as-quenched 4340 and 3.5NiCrMoV steels was studied under hydrogen charging conditions, with a cathodic current applied to the gauge length of specimens subjected to Linearly Increasing Stress Test (LIST) in 0.5 M H_2SO_4 solution containing 2 g/l arsenic trioxide (As_2O_3) at 30 °C. Applied stress rates were varied from 20.8 to 6×10^{-4} MPa s^{-1}. Both the fracture and threshold stress decreased with decreasing applied stress rate and were substantially lower than corresponding values measured in distilled water at 30 °C at the open circuit potential. The threshold stress values correspond to 0.03–0.08 σ_y for 4340 and 0.03–0.2 σ_y for the 3.5NiCrMoV steel. SCC velocities, at the same applied stress rate, were an order of magnitude greater than those in distilled water. However, the plots of the crack velocity versus applied stress rate had similar slopes, suggesting the same rate-limiting step. The fracture surface morphology was mostly intergranular, with quasi-cleavage features.

1. Introduction

Stress Corrosion Cracking (SCC) [1–4] occurs for a susceptible material subjected to a tensile stress in an aggressive environment and can lead to catastrophic failures [5–8]. High strength steels are particularly susceptible; increasing yield strength significantly decreases the threshold stress intensity factor, K_{ISCC} [9–11]. As a consequence, SCC of high strength steels has been widely studied [12–17] and is an on-going effort [3,5,18–20]. This paper follows our previous studies of the SCC of two high-strength steels (4340 and 3.5NiCrMoV) in distilled water at 90 °C [21] and 30 °C [22], which studied the influence of the applied stress rate on SCC using the Linearly Increasing Stress Test (LIST) [23–31]. These studies indicated that the SCC velocity increased with increasing applied stress rate until it reached a maximum SCC velocity; for 4340, the maximum SCC velocity corresponded to the plateau SCC velocity measured in fracture mechanics tests [32,33]. The SCC velocity was the same for both steels, indicating a similar rate-limiting step. The experiments in distilled water at 30 and 90 °C indicated that the same rate-limiting step could be operating at both temperatures. Nevertheless, the mechanism of SCC could be different at the two temperatures. It was suggested [21,32,34] that the SCC mechanism involved anodic dissolution at 90 °C. Anodic dissolution, in its simplest form, involves the dissolution of metal at the crack tip, which is kept bare by the crack tip strain rate. In contrast, it was thought [32,33] that hydrogen was involved at temperatures less than 60 °C, in which case a role of crack tip strain rate is to maintain a bare crack tip for easy hydrogen entry into the steel. High strength steels exhibit intergranular fracture along prior austenite grain boundaries and hence it is difficult to identify the SCC mechanism from the fracture surface morphology alone [35].

The present research was carried out to explore the behaviour of these steels under cathodic hydrogen charging conditions using LIST. The LIST tests were the same as in our previous studies [21,22] so that the cracking behaviour with cathodic hydrogen charging could be directly compared with the experimental results in distilled water at 30 and 90 °C.

2. Experimental procedure

Cylindrical tensile specimens were machined from 4340 and 3.5NiCrMoV rotor steel from the same steel plates as used in our previous studies [21,22]. Their composition is shown in Table 1. All 4340 specimens were austenitized at 860 °C in high purity nitrogen for 1 h and quenched into oil. A similar procedure was followed for the 3.5NiCrMoV steel. Batch heat-treatment ensured that the microstructure was the same for each specimen for each steel. The heat treatment resulted in a fully martensitic microstructure in both steels, with a prior austenite grain size of 20 μm, as described by Gates et al. [36]. The yield strength (σ_y) of 4340 was 1700 MPa and that of the 3.5NiCrMoV steel was 1270 MPa.

* Corresponding author at: Surface Science Western, The University of Western Ontario, London, Ontario, Canada N6G 0J3. Tel.: +1 519 661 2173; fax: +1 519 661 3709.
E-mail address: sramamur@uwo.ca (S. Ramamurthy).

0010-938X/$ - see front matter © 2011 Elsevier Ltd. All rights reserved.
doi:10.1016/j.corsci.2011.03.028

Table 1
Composition of the steels used in this study.

Steel	Composition (wt.%)								
	C	Ni	Cr	Mo	V	Mn	P	Si	S
4340	0.35	1.47	1.5	0.25	0.01	0.5	0.017	0.35	0.025
3.5NiCrMoV	0.23	3.05	1.9	0.65	0.07	0.45	0.011	–	0.009

After heat-treatment, each specimen was mounted in a lathe and the gauge section was ground through successive silicon carbide papers to 800 grit. Identical grinding conditions, including lathe speed, was employed for the preparation of each sample and, furthermore, the gauge section of each specimen was examined with optical microscopy after the grinding procedure to ensure that the gauge section surface was uniform and did not contain any coarse scratches or other surface defects that could act as crack initiation sites. The samples were then degreased in an ultrasonic cleaner with technical grade hexane solution, rinsed with distilled water and immediately loaded in the LIST apparatus.

The key to the LIST apparatus [23–31] is a lever beam. The specimen, and its loading train, is on one side of the lever beam and the other side contains a movable weight. Movement of the weight, driven by a synchronous motor, from its equilibrium position causes a proportional loading on the specimen, which is reported in terms of engineering stress. Synchronous motors of different speeds allowed nine applied stress rates, ranging from 0.0005 to 20 MPa s^{-1}.

For each LIST experiment, the steel was specimen immersed in 0.5 M H_2SO_4 solution containing 2 g/l arsenic trioxide (As_2O_3) at 30 °C as a hydrogen recombination poison. Each LIST specimen was subjected to a cathodic current of 0.5 A, resulting in a current density of 2600 A/m^2 on the gauge section. There was no surface damage or cracking on the tensile specimens in the as-charged condition without any applied stress. LISTs were conducted at 30 °C rather that at room temperature to ensure minimal variation in temperature. Once the desired temperature was reached, an hour was allowed for stabilisation and the cathodic current and stressing were applied. After fracture, the specimen was removed from the cell, washed with distilled water and dried. The fracture stress, σ_f, was calculated from the value of the load and the initial specimen cross-section area. The fracture surfaces were examined in a scanning electron microscope (SEM). Two identical samples were tested at each applied stress rate where there was SCC. Even at the low applied stress rates (0.0005 and 0.0006 MPa s^{-1}), where the duration of the tests could be a month or longer, repeat samples were used to determine the reproducibility of the measurements.

The SCC threshold stress, σ_{th}, was determined using a potential drop technique. During a LIST, a 5 A stabilised d.c. current (from a BWD model 245 A power supply) was applied to the specimen and the resulting potential drop across the specimen was plotted as a function of the applied stress. The threshold stress was identified as the stress at which there was a change in the slope in the potential drop versus applied stress plot, corresponding to a decrease in the cross-sectional area of the gauge section due to crack propagation. A CDP-10 linear displacement transducer (manufactured by Tokyo Sokki Kenkyujo Ltd.) was attached to the loading arms to measure the displacement of the specimen. This displacement was calibrated to give an output proportional to the specimen strain. The strain rate at the threshold stress was in each case determined from the slope of the strain versus time plot at the threshold stress; the threshold stress itself was evaluated from the potential drop measurements.

Assuming the SCC cracks grow at a constant rate between σ_{th} and σ_f, the average crack growth rate, v, was calculated from the following equation, where a is the maximum crack depth on the fracture surface after the test and $\dot{\sigma}$ is the applied stress rate [21,22]:

$$v = \frac{a\dot{\sigma}}{\sigma_f - \sigma_{th}} \quad (1)$$

The precision in the LIST tests were as follows. The total error in the specimen load was less than ±1% for loads of 1000 N and less than ±0.14% for higher loads [23]. The loading rate, determined by the speed of the synchronous motor, was accurate to ±1% [23]. The precision in the potential drop measurements was ±0.1 μV. Potential drop values were measured at every second for higher applied stress rates and at every few minutes for the low applied stress rates. The precision in the temperature control was better than ±1 °C. The error in the crack length measurements was ±0.1 mm [23].

3. Experimental results

3.1. Potential drop measurements

Figs. 1 and 2 present typical potential drop curves plotted against the applied stress for 4340 and 3.5NiCrMoV steel, respectively, subjected to LIST in 0.5 M H_2SO_4 + 2 g/l As_2O_3 solution under hydrogen charging conditions. The methodology employed during the potential drop measurements was the same as in previous studies [21,22]. Each number in Figs. 1 and 2 identifies the potential drop data for the LIST experiment with that same number in Figs. 3 and 4, respectively. Arrows in these figures marked the point at which there was a change in slope in the potential drop-applied stress plot. The stress at this point was identified as the threshold stress and plotted in Figs. 3 and 4.

3.2. Fracture stress and threshold stress

The threshold stress and the fracture stress for as-quenched 4340 under hydrogen charging conditions in 0.5 M H_2SO_4 + 2 g/l As_2O_3 solution at 30 °C are plotted in Fig. 3 as a function of applied stress rate. The symbols represent the experimental data and the black solid lines represent the polynomial regression fit for the data. SCC was observed at all applied stress rates shown in the figure. Moreover, both the fracture and threshold stresses decreased with decreasing applied stress rate. The fracture and threshold stress values were low. The fracture stress varied from ~200 to

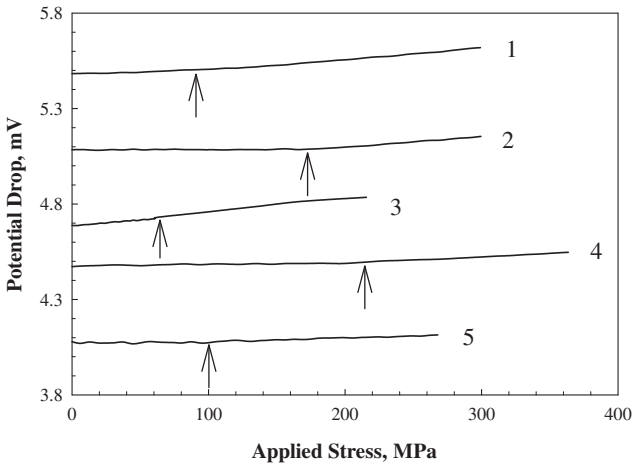

Fig. 1. A plot of the potential drop as a function of the applied stress for representative tests with as-quenched 4340. The arrows represent the change in the slope of potential drop plot and mark the threshold stress corresponding to crack initiation. Numbers 1–5 correspond to the data points shown in Fig. 3.